



A comparative density functional theory study of the direct synthesis of H_2O_2 on Pd, Pt and Au surfaces

R. Todorovic, R.J. Meyer*

Department of Chemical Engineering, University of Illinois at Chicago, 810 S Clinton, Chicago, IL 60607, United States

ARTICLE INFO

Article history:

Available online 21 August 2010

Keywords:

Hydrogen peroxide
Gold
Palladium
Alloys
Density functional theory
Oxygen
Hydrogen

ABSTRACT

The direct synthesis of hydrogen peroxide (H_2O_2) from hydrogen (H_2) and oxygen (O_2) on Pd(1 1 1), Pt(1 1 1), PdH(2 1 1) and $\text{Au}_{0.89}\text{Pd}_{0.11}$ (2 2 1) catalysts was investigated through the use of Density Functional Theory calculations. Three formation steps and their competing (decomposition) counterparts were examined on all model surfaces: O_2 hydrogenation versus O_2 dissociation, OOH hydrogenation versus OOH dissociation, and H_2O_2 desorption versus H_2O_2 dissociation. We have found that as we change the surface from Pd to Pt to Au, the step which governs the non-selective formation of water shifts from O_2 dissociation to OOH dissociation to H_2O_2 decomposition.

© 2010 Elsevier B.V. All rights reserved.

1. Introduction

Hydrogen peroxide is a key commodity chemical that has large-scale use as a cleansing agent and as a selective oxidant in the fine chemical industry [1]. Currently the majority of selective or partial oxidation processes use bulky stoichiometric organic donors that exhibit poor atom efficiency. Hydrogen peroxide is the next preferred green oxidant, after O_2 , because the byproduct after oxygen donation is water. At present no commercial process exists that produces hydrogen peroxide via the direct hydrogenation of molecular oxygen with hydrogen, as industrial production of H_2O_2 is performed using a Riedl–Pfleiderer process, an indirect anthraquinone process. Development of a direct synthesis route to hydrogen peroxide is of significant commercial interest, as safety issues stemming from an inability to produce hydrogen peroxide on site in desirable concentrations (3–8%) prevent larger scale use in the chemical industry.

The main focus of early experimental studies was to achieve high rates of product formation [2]. The solutions of greater than 35 wt% hydrogen peroxide were made by reacting H_2 and O_2 mixtures typically over palladium catalysts at elevated pressure of approximately 10 MPa and temperatures in range of 0–50 °C [3]. Using an aqueous medium, explosion hazards associated with the combination of high H_2O_2 concentrations and organic cosolvents are absent. However, there is still an intrinsic hazard associated with mixing H_2 and O_2 gases at high pressures over a supported metal

oxidation catalyst as the non-selective formation of water is highly exothermic and potentially explosive. Therefore, studies have been performed that utilize feed-streams containing hydrogen concentration of less than 4 vol% wherein due to a dilute nature of the mixture the process will be carried out away from the explosive region [4]. However, the biggest issue associated with a direct H_2O_2 synthesis process is the selectivity, because conditions suitable for the synthesis of H_2O_2 are the same leading to its dissociation or to a non-selective formation of H_2O .

Although competitive selectivities can be achieved with halide promoted Pd catalysts [5], handling the aqueous phase promoters is problematic due to waste generation. As an improvement to Pd monometallic catalysts, Hutchings and co-workers [6] have found that PdAu catalysts are both active and selective for H_2O_2 formation even without the presence of additional promoters. Calcination was found to be critical to the stability of the catalyst and selectivities of larger than 90% could be achieved. Active PdAu catalysts were found to be enriched in Pd at the surface. Recently, Hutchings and co-workers [7] have further improved on this process. Using an acid pretreatment on a carbon support of AuPd alloy catalyst they were able to completely block H_2O_2 hydrogenation and decomposition and selectivity to H_2O_2 of 98% can be achieved. Unlike AuPd nanoparticles on oxide supports, the alloy particles on carbon tend to be homogenous as opposed to core-shell. However, acid pretreatment of the support improved nanoparticle nucleation and thereby favored the formation of a greater number fraction of the smallest (which are Pd-rich) alloy particles as opposed to intermediate (Au–Pd, 1:1) or large (Au-rich) particles. With some additional gains in performance, commercialization of these catalysts may soon be possible.

* Corresponding author. Tel.: +1 312 996 4607.

E-mail address: rjm@uic.edu (R.J. Meyer).

The demand for improvement of the catalyst selectivity in the direct synthesis of H_2O_2 has inspired some recent theoretical investigations concerning the mechanism of the reaction and the steps which control selectivity [8–10]. Staykov et al. [10] have examined the hydrogenation of O_2 and OOH on Pd(1 1 1) and gold substituted Pd and found that for Pd(1 1 1), OOH hydrogenation will be the limiting step in H_2O_2 synthesis, causing a non-selective formation of water. By substituting two Pd atoms with Au atoms in the Pd(1 1 1) surface, the barrier to dissociation of O_2 increases from 0.88 eV to 1.38 eV and should therefore increase the selectivity for H_2O_2 formation. However, in Staykov et al.'s work, the authors did not consider the dissociation of OOH or the decomposition of H_2O_2 . Hwang and co-workers [8] observed that the selectivity of direct H_2O_2 synthesis is directly related to the amount of Au in the surface. The barriers for dissociation reactions increase as the amount of Au in the surface increases. Similarly, the barriers for the hydrogenation reactions (which are associative) decrease as the amount of Au in the surface increases. This would indicate that a surface which is nearly covered with Au should be a highly selective H_2O_2 synthesis catalyst. However, molecular oxygen does not adsorb strongly to Au and the presence of Au should also suppress H_2 dissociation. As Barrio et al. [11] have previously established, molecular H_2 will not adsorb on Au(1 1 1) and Au(1 0 0) surfaces.

The aim of this study is to perform further theoretical examination of candidate surfaces that may increase the selectivity towards the main product, H_2O_2 . Four different catalytic surfaces, Pd(1 1 1), Pt(1 1 1), PdH(2 1 1) and $Au_{0.89}Pd_{0.11}(2 2 1)$, were investigated for the selective direct formation of H_2O_2 from molecular H_2 and O_2 . Four possible reaction mechanisms on each candidate surface were examined: the desired path to H_2O_2 formation and three competing mechanisms, O_2 intermediate dissociation path to H_2O , hydroperoxo intermediate dissociation path to H_2O , and the H_2O_2 decomposition. The complete potential energy surface for each of these reaction pathways has been calculated including transition state barriers for the desired process as well as its competing counterparts in order to determine the important steps and the factors that will influence the selectivity. Our goal is to perform a detailed analysis of prior investigated surfaces as well as to explore some possible new candidates for the safe and efficient synthesis of H_2O_2 . We have found that as we change the surface from Pd to Pt to Au, the step which governs the non-selective formation of water shifts from O_2 dissociation to OOH dissociation to H_2O_2 decomposition.

2. Methods

The density functional theory calculations in this work are performed using the Vienna *Ab Initio* Simulation package (VASP) [12,13]. A plane-wave basis set with a cutoff energy of 400 eV and ultrasoft Vanderbilt pseudopotentials (U.S.-PP) [14] were employed. The Perdew Wang (PW-91) form of the generalized gradient approximation (GGA) exchange [15] and correlation functional was used in all calculations reported herein.

For the Pd(1 1 1), Pt(1 1 1), and Au(2 2 1) a 3×3 unit cells with four layer thick metal slabs were used for all calculations. The bottom two layers of metal were held fixed while the top metal layers and the adsorbates were relaxed. Vacuum space equivalent to approximately four atomic layers was used to separate the slabs. For PdH(2 1 1) a five (metal) layer thick metal hydride was used, keeping the subsurface H layer empty. The slab was cleaved from the bulk geometry of β -PdH_{0.8}, which possesses a tetragonal unit cell [16]. The bottom two metal layers were held fixed while the top three metal layers and the adsorbates were relaxed. The H-vacancy structure results from the migration of the top H atom in the Pd-terminated surface towards the adsorption position, leaving behind the vacancy between the two top Pd layers

<i>H₂O₂ Formation</i>	<i>O₂ Intermediate Dissociation Path to H₂O</i>
$H_2(g) + O_2(g) \rightarrow 2H^* + O_2^*$	$H_2(g) + O_2(g) \rightarrow 2H^* + O_2^*$
$2H^* + O_2^* \rightarrow H^* + OOH^*$	$2H^* + O_2^* \rightarrow 2H^* + 2O^*$
$H^* + OOH^* \rightarrow H_2O_2^*$	$2H^* + 2O^* \rightarrow OH^* + H^* + O^*$
$H_2O_2^* \rightarrow H_2O_2(g)$	$OH^* + H^* + O^* \rightarrow H_2O^* + O^*$
<i>Hydroperoxo Intermediate Dissociation Path to H₂O</i>	<i>H₂O₂ Decomposition</i>
$H_2(g) + O_2(g) \rightarrow 2H^* + O_2^*$	$H_2(g) + O_2(g) \rightarrow 2H^* + O_2^*$
$2H^* + O_2^* \rightarrow H^* + OOH^*$	$2H^* + O_2^* \rightarrow H^* + OOH^*$
$H^* + OOH^* \rightarrow OH^* + O^* + H^*$	$H^* + OOH^* \rightarrow H_2O_2^*$
$OH^* + O^* + H^* \rightarrow H_2O^* + O^*$	$H_2O_2^* \rightarrow 2OH^*$

Fig. 1. Summary of the reaction mechanisms examined.

and is represented by slabs of alternating layers of H and Pd. Discussion of this model is detailed in Section 3. The Brillouin zone was sampled with $(5 \times 5 \times 1)$ *k*-point grid (Monkhorst-Pack) [17]. Structures were converged with regard to both *k* points and cutoff energies to within 0.02 eV/adsorbate atoms (O and H). Finally, the energies of all molecules (H_2O_2 , O_2 , etc.) were calculated using a single molecule in a 10 Å cube with gamma point sampling.

Reaction paths and barriers are determined using the Climbing Nudged Elastic Band (NEB) method [18]. In the NEB method a reaction coordinate relating the initial and final states are defined and a set of intermediate states are distributed along the reaction path. Each intermediate state is fully relaxed in the hyperspace perpendicular to the reaction coordinate. Vibrational frequencies were computed for the initial, transition and final states, where the substrate is frozen but adsorbates are allowed to vibrate in any direction. If the molecule is in a true transition state it should have one and only one imaginary frequency. Vibrational frequencies were also used to perform zero point vibrational energy corrections to all the relevant initial, transition and final states.

3. Results and discussion

The direct synthesis of hydrogen peroxide from hydrogen and oxygen occurs through the hydrogenation of molecular oxygen on the surface as shown in Fig. 1. However, as mentioned above, three alternative pathways exist that all result in the non-selective production of water. First, O_2 may dissociate prior to hydrogenation. Oxygen atoms may then be hydrogenated to form OH species and ultimately, H_2O . Second, the hydroperoxo intermediate (OOH) which is formed after the first hydrogenation step in H_2O_2 synthesis may dissociate into OH and O surface species before the second hydrogenation step. The surface OH species are then hydrogenated to form H_2O . Finally, even if O_2 is successfully hydrogenated to form peroxide, H_2O_2 may dissociate, prior to desorption, into two OH surface species which can subsequently react via disproportionation to form water. We have calculated the thermodynamics and kinetics for all the steps in Fig. 1 over four surfaces of interest: Pd(1 1 1), Pt(1 1 1), PdH(2 1 1) and $Au_{0.89}Pd_{0.11}(2 2 1)$ with all relevant reaction enthalpies and barriers listed in Table 1. We will discuss the kinetically relevant steps for each surface in turn beginning with Pd(1 1 1).

Clearly O_2 must be adsorbed molecularly (without dissociating) on the metal surface before H_2O_2 can be produced. Therefore, it is imperative that an active, selective H_2O_2 synthesis catalyst will have a high barrier to O_2 dissociation. Honkala and Laasonen [9] have previously studied O_2 adsorption and dissociation on the Pd(1 1 1) surface using DFT. On Pd(1 1 1), O_2 may adsorb molecularly to a bridge site (−0.95 eV) which is a precursor state for the O_2

Table 1

Summary of the activation energies (E_{act}) and reaction enthalpies (ΔH) for the O_2 hydrogenation and dissociation, OOH hydrogenation and dissociation, O and OH hydrogenation, and H_2O_2 decomposition reactions on four surfaces of interest (energies are referenced to the initial states and are reported in eV).

Reactions	Pd(1 1 1)		Pt(1 1 1)		PdH(2 1 1)		AuPd(2 2 1)	
	E_{act}	ΔH	E_{act}	ΔH	E_{act}	ΔH	E_{act}	ΔH
$\text{O}_2 + 2\text{H} \rightarrow \text{OOH} + \text{H}$	0.75	0.41	0.60	−0.09	0.51	0.20	0.19	−0.76
$\text{H} + \text{OOH} \rightarrow \text{HOOH}$	1.13	0.37	0.91	0.04	0.73	0.34	0.70	−0.39
$\text{O}_2 + 2\text{H} \rightarrow 2\text{O} + 2\text{H}$	0.59	−1.44	0.89	−0.87	0.77	−1.05	1.81	0.59
$\text{H} + \text{OOH} \rightarrow \text{OH} + \text{H} + \text{O}$	0.35	−1.51	0.05	−1.25	0.12	−1.48	0.72	−0.49
$\text{HOOH} \rightarrow 2\text{OH}$	0.04	−1.64	0.03	−1.37	0.05	−1.73	0.09	−1.63
$2\text{O} + 2\text{H} \rightarrow \text{OH} + \text{H} + \text{O}$	0.72	0.34	1.41	−0.48	0.87	−0.10	0.34	−1.66
$\text{OH} + \text{H} + \text{O} \rightarrow \text{H}_2\text{O} + \text{O}$	0.42	−0.58	0.26	−0.67	0.49	−0.26	0.02	−1.00

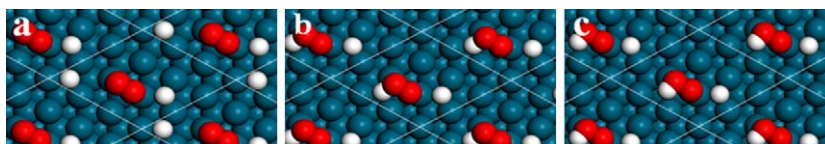


Fig. 2. O_2 hydrogenation reaction: (a) top view of initial ($\text{O}_2 + 2\text{H}$), (b) transition and (c) final ($\text{OOH} + \text{H}$) states.

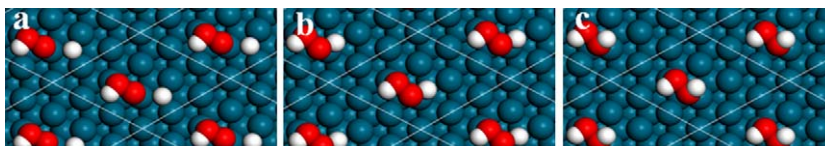


Fig. 3. Hydroperoxo hydrogenation reaction: (a) top view of initial ($\text{OOH} + \text{H}$), (b) transition and (c) final (H_2O_2) states.

adsorption. We have calculated the adsorption and dissociation for O_2 on Pd(1 1 1) and have found that for 0.5 ML coverage activation energy is 0.77 eV [19] in agreement with results from Honkala and Laasonen [9] and Hafner and co-workers [20].

In contrast to oxygen, hydrogen must adsorb dissociatively with a low barrier. Hafner and co-workers [21] found that threefold-hollow fcc sites are the most stable sites for the dissociative adsorption of H_2 on Pd(1 1 1), reporting a hydrogen adsorption energy of -0.50 eV for the $2/3$ ML coverage with no barrier. Hence, these results show that Pd(1 1 1) can dissociate H_2 molecules quite efficiently. Our own calculations confirm these findings as we could locate no barrier to dissociative H_2 adsorption ($\Delta E = -0.91$ eV).

Following O_2 adsorption, H_2O_2 formation proceeds through two consecutive hydrogenation reactions as depicted in Figs. 2 and 3, followed by the H_2O_2 desorption. Both hydrogenation reactions on the Pd(1 1 1) surface are thermoneutral. While the initial hydrogenation barrier is 0.75 eV (Fig. 2), the second reaction has a 1.13 eV (Fig. 3) barrier, which leads to low selectivity. H_2O_2 , once formed, is weakly bound to the surface with adsorption energy of -0.38 eV.

Along the path described above, there are several other deleterious reactions which can decrease selectivity to H_2O_2 . First, O_2 may also dissociate to 2 O atoms located at fcc sites with a barrier of 0.59 eV on Pd(1 1 1) as depicted in Fig. 4. Second, the OOH intermediate formed after the initial hydrogenation step may dissociate to $\text{OH} + \text{O}$ on the surface with a barrier of 0.35 eV as shown in Fig. 5. Finally, as shown in Fig. 6, decomposition of H_2O_2 may occur prior to desorption. Hydrogen peroxide may dissociate into two

OH's which is spontaneous with no discernable energy barrier. In the case of Pd(1 1 1), the barrier to O_2 dissociation is 0.16 eV smaller than that for hydrogenation to OOH. In Fig. 7, the entire reaction pathway for H_2O_2 formation on Pd(1 1 1) is depicted. As the barrier for first hydrogenation reaction is larger than the barrier for O_2 dissociation, this step governs a non-selective formation of water. This result is not surprising given that experimental results clearly indicate that unpromoted Pd is unselective for hydrogen peroxide formation.

From previous work of Norskov and co-workers [22–25], we note that the high reactivity of the Pd(1 1 1) surface to O_2 dissociation is related to the location of the d -band center. Therefore, if we move to a less reactive metal, O_2 dissociation may be suppressed and association reactions like O_2 hydrogenation may be favored. Therefore, we have chosen Pt(1 1 1) as a second candidate surface for our analysis of direct synthesis of H_2O_2 . The potential energy surface for H_2O_2 formation over Pt(1 1 1) is shown in Fig. 8. As in the case for Pd(1 1 1), we have found that hydrogen dissociation is barrierless over Pt(1 1 1) in agreement with previous calculations [26]. The barrier for O_2 dissociation over Pt(1 1 1) rises to 0.89 eV. At the same time, we found a barrier for the initial hydrogenation reaction to be 0.60 eV, thus indicating that OOH formation should precede on Pt(1 1 1). In our calculation of the second hydrogenation barrier (0.91 eV) on Pt(1 1 1), once again we find that it is more difficult than the initial hydrogenation step. However, unlike O_2 which is a stable gas phase molecule, OOH is a highly reactive surface intermediate and possesses a low barrier of 0.06 eV to dissociate to O and OH on the Pt(1 1 1) surface. Therefore, although the unselective

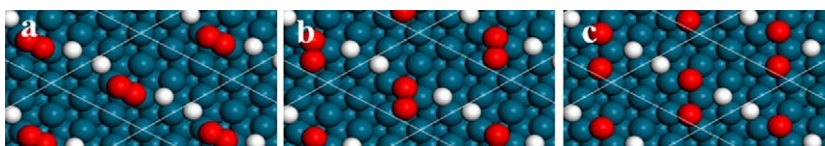


Fig. 4. O_2 dissociation reaction: (a) top view of initial ($\text{O}_2 + 2\text{H}$), (b) transition and (c) final ($2\text{O} + 2\text{H}$) states.

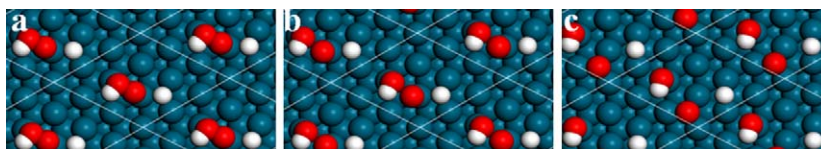


Fig. 5. Hydroperoxo dissociation reaction: (a) top view of initial (OOH + H), (b) transition and (c) final (OH + O + H) states.

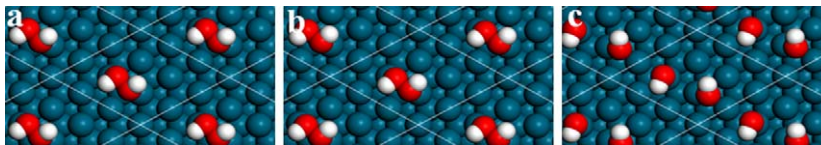


Fig. 6. Hydroperoxo decomposition reaction: (a) top view of initial (H_2O_2), (b) transition and (c) final (2 OH) states.

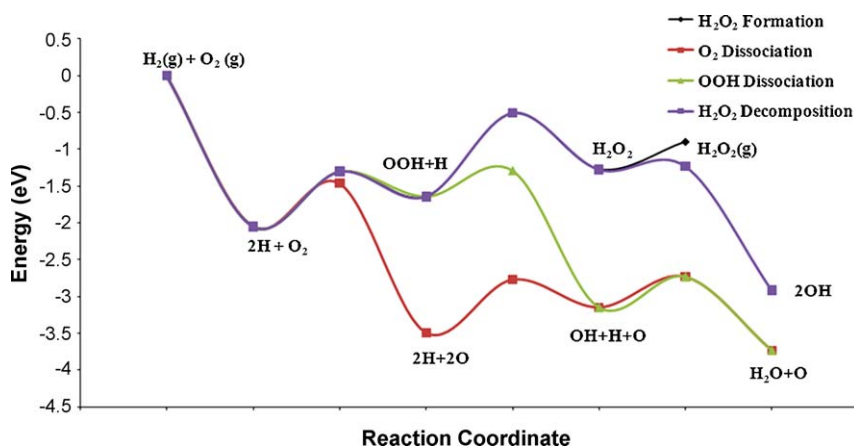


Fig. 7. Potential energy surface for the reaction mechanisms on Pd (1 1 1). Activation barriers and reaction mechanism species are plotted with reference to the gas phase H_2 and O_2 .

tive product, H_2O , is again preferred, the rate limiting step which controls its formation has now switched from the dissociation of O_2 on Pd(1 1 1) to the dissociation of OOH on Pt(1 1 1).

One well known feature of Pd hydrogenation catalysts is that hydrogen may diffuse into the subsurface forming palladium hydride [27]. Even at the very low partial pressure of H, Pd will react to form PdH [28,29]. Therefore, given the hydrogen partial pressures often involved in direct hydrogen peroxide synthesis, a model of the PdH surface was constructed to give some insight into the presence of subsurface hydrogen on the reaction selectivity. Our model of $\beta\text{-PdH}(2\ 1\ 1)$ follows that previously developed in the

DFT calculations of King and co-workers [30]. King and co-workers created a 1:1 PdH structure by placing hydrogen into all of the octahedral sites of the Pd bulk where the Pd lattice is expanded by 4% by the presence of hydrogen. They showed that H in the adsorption position (H-vacancy configuration) is more stable by 0.33 eV, as compared to the Pd-terminated surface configuration. Our own model of the PdH(2 1 1) surface follows that of King et al. where we use the tetragonal unit cell $\text{PdH}_{0.8}$ so that 80% of the octahedral sites in the bulk are occupied. Therefore, the first surface we examined was the so-called H-vacancy surface, whereby one monolayer of hydrogen atoms sits on the surface with no hydro-

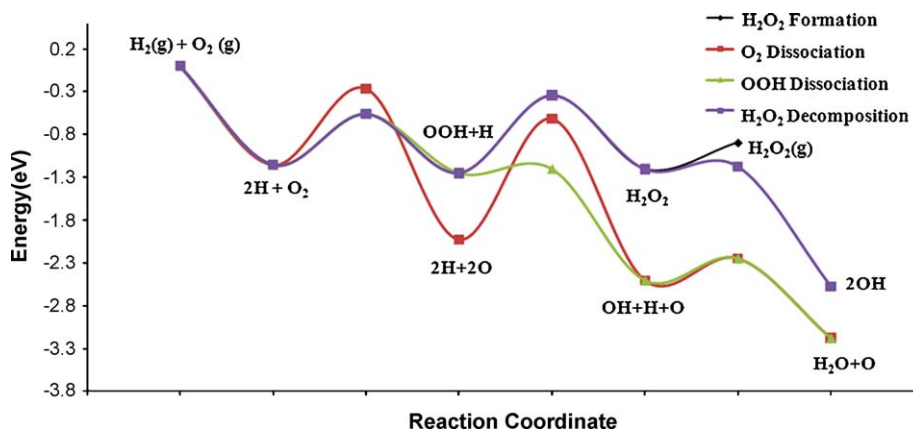


Fig. 8. Potential energy surface for the reaction mechanisms on Pt (1 1 1). Activation barriers and reaction mechanism species are plotted with reference to the gas phase H_2 and O_2 .

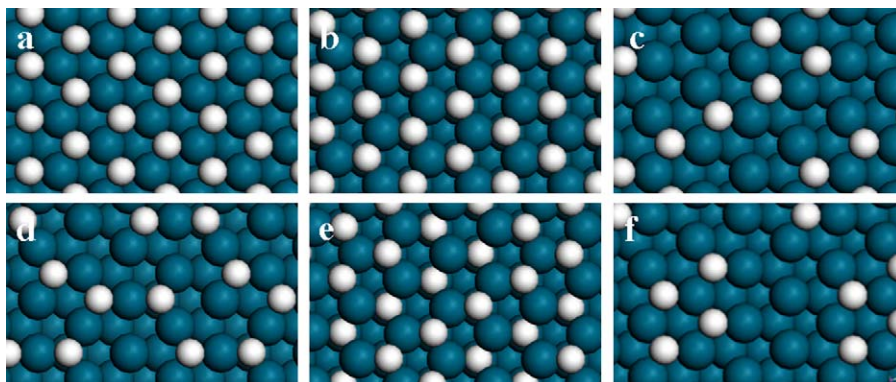


Fig. 9. PdH(2 1 1) surfaces examined: (a) H-vacancy/FCC, (b) H-vacancy/HCP, (c) H-vacancy/0.5 ML H/FCC, (d) H-vacancy/0.5 ML H/HCP, (e) 0.5 ML H/HCP + 0.5 ML octahedral, (f) H-vacancy/0.4 ML H/FCC.

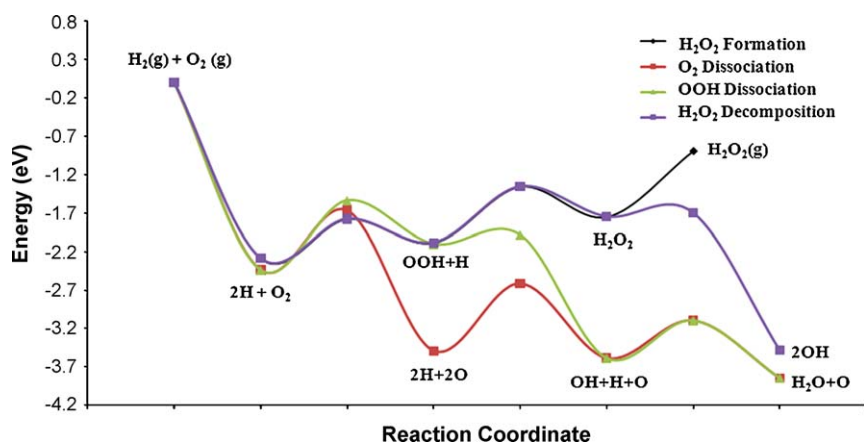


Fig. 10. Potential energy surface for the reaction mechanisms on H-vacancy/0.4 ML H/FCC PdH(2 1 1). Activation barriers and reaction mechanism species are plotted with reference to the gas phase H_2 and O_2 .

gen present in the first subsurface layer as depicted in Fig. 9a. As in the case of Pd(1 1 1), hydrogen spontaneously dissociates on open locations of the metal hydride surface. The possibility of H adsorption onto two different surface (and subsurface) threefold hollow sites, FCC (octahedral) and HCP (tetrahedral), requires a need to test different surfaces in search for the lowest energy configuration. Four additional PdH(2 1 1) surfaces were examined: an HCP H-vacancy surface (Fig. 9b), an FCC surface with 0.5 ML H (Fig. 9c), an HCP surface with 0.5 ML H (Fig. 9d), and a surface combining the HCP structure with 0.5 ML H in octahedral sites (Fig. 9e). Results obtained by King and co-workers [30] were confirmed showing that the H-vacancy terminated surface is the thermodynamically most stable system under UHV and that it gives the lowest energy configuration. However, it was found that oxygen could not adsorb on any of the surfaces where a full monolayer of hydrogen atoms was preadsorbed (Fig. 9a, b and e) and in fact, O_2 adsorption was very weak on the surfaces with 0.5 ML of hydrogen atoms. Therefore in order to stabilize molecular oxygen in a state where it can be hydrogenated, the hydrogen coverage must be reduced to 0.4 ML surface coverage. Although this coverage is somewhat arbitrary, we have chosen to examine it as a limiting case: the highest hydrogen coverage which allows adsorption of molecular oxygen. One can imagine that in real systems, there may be local regions which are hydrogen deficient and therefore we have chosen this surface with this idea in mind.

The 0.4 ML H-covered PdH(2 1 1) surface is depicted in Fig. 9f. O_2 adsorbs exothermically on this surface (-0.6 eV), but the barrier to dissociation rises from 0.59 eV to 0.77 eV. As depicted in Fig. 10, the lowest energy path follows a mechanism by which O_2 is hydrogenated with a barrier of 0.52 eV (0.26 eV lower than

O_2 dissociation) but OOH dissociates easily on the surface just as it is the case with Pt(1 1 1). When the PdH(2 1 1) activation energies for each of the reaction mechanisms is compared to those on Pd(1 1 1) and Pt(1 1 1), it can be concluded that the PdH(2 1 1) surface will increase the O_2 and OOH dissociation barriers and lower the hydrogenation barriers. However, our calculations show that the palladium hydride surface still does not result in a selective surface for H_2O_2 formation.

As mentioned above, Barrio et al. found that low index surfaces of Au do not activate H_2 [11]. However, Barrio did observe that H_2 could dissociate spontaneously on Au_{14} and Au_{29} clusters. Therefore, we chose to examine a stepped gold surface where the

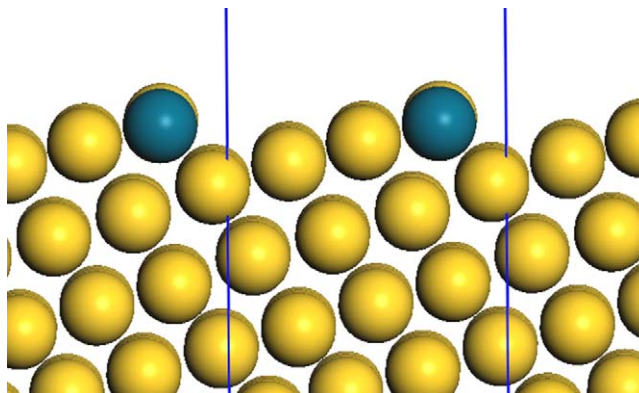


Fig. 11. Side view of the AuPd(2 2 1) surface.

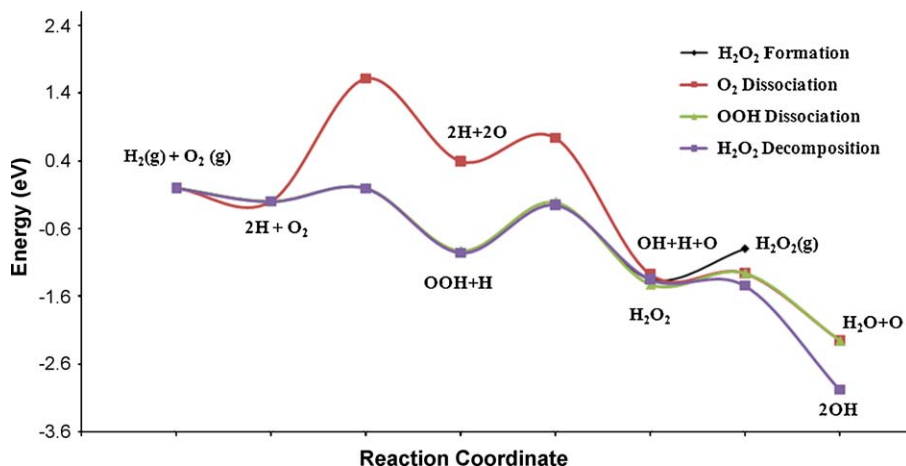


Fig. 12. Potential energy surface for the reaction mechanisms on $\text{Au}_{0.89}\text{Pd}_{0.11}(2\ 2\ 1)$. Activation barriers and reaction mechanism species are plotted with reference to the gas phase H_2 and O_2 .

barrier to hydrogen dissociation may be sufficiently low to allow reaction between hydrogen atoms and O_2 . After examining three possible step adsorption sites (threefold, bridge-above edge and bridge-side edge site) we have found that the hydrogen dissociation is thermoneutral with a -0.01 eV adsorption energy and a barrier of 0.80 eV. Given this limitation, it appears that the $\text{Au}(2\ 2\ 1)$ cannot be active for direct hydrogenation of O_2 to H_2O_2 .

As mentioned above, AuPd alloys have been demonstrated to be successful for hydrogen peroxide synthesis. Results from Ham et al. [8], indicate that even the presence of isolated Pd atoms in a gold surface will increase its activity sufficiently to create a viable catalytic surface with high selectivity. Based upon our result for $\text{Au}(2\ 2\ 1)$ and the results of Ham et al., we have then decided to examine an analogous situation by replacing a single atom of Au in the $\text{Au}(2\ 2\ 1)$ step with Pd as shown in Fig. 11. As in the case of the Au substituted $\text{Pd}(1\ 1\ 1)$, surface created by Ham et al. [8], the $\text{Au}_{0.89}\text{Pd}_{0.11}(2\ 2\ 1)$ step surface was found to be highly selective towards the H_2O_2 surface species formation. Addition of one palladium atom to the step surface was sufficient to stabilize the adsorption of molecular O_2 on the surface. Different O_2 adsorption positions were examined and it was found that the exothermic adsorption of O_2 species is at the bridge site (-0.07 eV) above the Pd and an Au atom. This adsorption position was used as a starting geometry for all the reaction mechanisms on $\text{Au}_{0.89}\text{Pd}_{0.11}(2\ 2\ 1)$ surface. The potential energy surface for H_2O_2 formation over $\text{Au}_{0.89}\text{Pd}_{0.11}(2\ 2\ 1)$ is shown in Fig. 12. Lower activation barriers were found for all the desired reaction mechanism steps; therefore the selectivity towards the main product was increased. Over $\text{Au}_{0.89}\text{Pd}_{0.11}(2\ 2\ 1)$, the barrier for O_2 dissociation rises to 1.81 eV while hydrogen can more easily dissociate over the Pd substituted $\text{Au}(2\ 2\ 1)$ surface (0.47 eV). Unlike the $\text{Au}(2\ 2\ 1)$ surface, hydrogen adsorption is weakly exothermic on the $\text{Au}_{0.89}\text{Pd}_{0.11}(2\ 2\ 1)$ surface (-0.25 eV) but its dissociation is still essentially thermoneutral ($\Delta E = 0.05$ eV). At the same time, the O_2 hydrogenation barrier is decreased to 0.19 eV as OOH formation is considerably exothermic ($\Delta E = -0.76$ eV). For the OOH hydrogenation we find the barrier of 0.70 eV as compared to 0.72 eV for the dissociation, indicating the formation of H_2O_2 on the $\text{Au}_{0.89}\text{Pd}_{0.11}(2\ 2\ 1)$ surface. However, the selectivity issue arises once the surface H_2O_2 is formed. The energy barrier for H_2O_2 desorption is 0.45 eV, compared to the minimal energy barrier (0.09 eV) for the dissociation into 2 surface OH species. Therefore, once the H_2O_2 is formed it will spontaneously dissociate. Although the unselective product, H_2O will again be preferred through the

subsequent OH disproportionation reaction, the rate limiting step which controls its formation will be shifted from OOH dissociation to H_2O_2 decomposition. By comparison, we find that H_2O_2 dissociation over the pure gold surface of $\text{Au}(2\ 2\ 1)$ has a barrier of 0.25 eV surprisingly similar to the result of Ham et al. on $\text{Au}(1\ 1\ 1)$ (0.31 eV).

It should be noted that this study did not explicitly consider entropic effects. However, we can note that the free energy sacrifice for moving an oxygen molecule to the surface is 0.39 eV and for moving a hydrogen molecule to the surface is 0.30 eV using the reaction condition described in Edwards et al. [6] (not including any entropy associated with the mixture). Previously, O'Sullivan et al. report a free energy of solvation for H_2O_2 in an aqueous environment of ~ -28 kJ/mol (-0.29 eV) [31]. In addition, H_2O_2 has a free energy in the gas phase at the vapor pressure above an aqueous solution as described in Edwards et al. [6] of -0.71 eV. Considering these entropic effects, desorption of H_2O_2 from the metal surface where it can be dissolved into solution is a thermodynamically favorable process. However, the situation is slightly more complicated. In order to properly account for the solvent, the presence of water associated with the surface must be included in transition state in the hydrogenation process. Recently, Neurock and co-workers showed that the polarity of the transition state may vary considerably and thus the presence of the solvent may influence individual reaction barriers to a largely varying extent [32]. Therefore, a more complete study of solvent effects would be a valuable contribution for improved understanding of H_2O_2 production (and decomposition) on metal surfaces.

4. Conclusions

We have found that as we change the surface from Pd to Pt to Au, the step which governs the non-selective formation of water shifts from O_2 dissociation to OOH dissociation to H_2O_2 decomposition. Pure metal surfaces (Pd and Pt) exhibit low selectivity towards the product and in both cases the intermediate mechanism leading towards the non-selective formation of water was found. The β - $\text{PdH}(2\ 1\ 1)$ surface increases the O_2 dissociation barrier and lower the hydrogenation barriers. However, the dissociation of OOH is still favored over hydrogenation to H_2O_2 . $\text{Au}_{0.89}\text{Pd}_{0.11}(2\ 2\ 1)$ surface increases the selectivity for the H_2O_2 formation and more easily activates H_2 as compared to $\text{Au}(2\ 2\ 1)$ (and $\text{Au}(1\ 1\ 1)$ as well). However, the barrier to H_2O_2 dissociation is still too low to explain the experimentally observed selectivity.

Acknowledgments

RM acknowledges funding for this work from the American Chemical Society Petroleum Research Fund Grant #46131-G-5. RT acknowledges support from the National Science Foundation REU (CBET-0747646). RM and RT acknowledge grant of computer time from the Center for Nanoscale Materials at Argonne National Lab (Grant #753).

References

- [1] K.H. Buchel, H.H. Moretto, P. Woditsch, *Industrial Inorganic Chemistry*, Wiley-VCH, Weinheim, 2000.
- [2] J.H. Lunsford, *J. Catal.* 216 (2003) 455–460.
- [3] L.W. Gosser, J.A.T. Schwartz, Catalytic process for making hydrogen peroxide from hydrogen and oxygen employing a bromide promoter, US, 1988.
- [4] B. Zhou, L.K. Lee, Catalyst and process for direct catalytic production of hydrogen peroxide, No. 6168775, US, 2001.
- [5] Q.S. Liu, J.C. Bauer, R.E. Schaak, J.H. Lunsford, *Angew. Chem. Int. Ed.* 47 (2008) 6221–6224.
- [6] J.K. Edwards, B.E. Solsona, P. Landon, A.F. Carley, A. Herzing, C.J. Kiely, G.J. Hutchings, *J. Catal.* 236 (2005) 69–79.
- [7] J.K. Edwards, B. Solsona, E.N.N.A.F. Carley, A.A. Herzing, C.J. Kiely, G.J. Hutchings, *Science* 323 (2009) 1037–1041.
- [8] H.C. Ham, G.S. Hwang, J. Han, S.W. Nam, T.H. Lim, *J. Phys. Chem. C* 113 (2009) 12943–12945.
- [9] K. Honkala, K. Laasonen, *J. Chem. Phys.* 115 (2001) 2297–2302.
- [10] A. Staykov, T. Kamachi, T. Ishihara, K. Yoshizawa, *J. Phys. Chem. C* 112 (2008) 19501–19505.
- [11] L. Barrio, P. Liu, J.A. Rodriguez, J.M. Campos-Martin, J.L.G. Fierro, *J. Chem. Phys.* 125 (2006) 164715.
- [12] G. Kresse, J. Furthmuller, *Phys. Rev. B* 54 (1996) 11169–11186.
- [13] G. Kresse, J. Furthmuller, *Comput. Mater. Sci.* 6 (1996) 15–50.
- [14] D. Vanderbilt, *Phys. Rev. B* 41 (1990) 7892–7895.
- [15] J.P. Perdew, Y. Wang, *Phys. Rev. B* 45 (1992) 13244–13249.
- [16] E. Wu, S.J. Kennedy, E.M.A. Gray, E.H. Kisi, *J. Phys.-Condens. Mater.* 8 (1996) 2807–2813.
- [17] H.J. Monkhorst, J.D. Pack, *Phys. Rev. B* 13 (1976) 5188–5192.
- [18] G. Henkelman, B.P. Uberuaga, H. Jonsson, *J. Chem. Phys.* 113 (2000) 9901–9904.
- [19] J. Jelic, R.J. Meyer, *Catal. Today* 136 (2008) 76–83.
- [20] A. Eichler, F. Mittendorfer, J. Hafner, *Phys. Rev. B* 62 (2000) 4744–4755.
- [21] W. Dong, J. Hafner, *Phys. Rev. B* 56 (1997) 15396–15403.
- [22] B. Hammer, J.K. Nørskov, *Surf. Sci.* 343 (1995) 211–220.
- [23] J.R. Kitchin, J.K. Nørskov, M.A. Barteau, J.G. Chen, *J. Chem. Phys.* 120 (2004) 10240–10246.
- [24] B. Hammer, J.K. Nørskov, *Adv. Catal.* 47 (45) (2000) 71–129.
- [25] J. Greeley, J.K. Nørskov, M. Mavrikakis, *Annu. Rev. Phys. Chem.* 53 (2002) 319–348.
- [26] R.A. Olsen, H.F. Busnengo, A. Salin, M.F. Somers, G.J. Kroes, E.J. Baerends, *J. Chem. Phys.* 116 (2002) 3841–3855.
- [27] A. Pundt, R. Kirchheim, *Ann. Rev. Mater. Res.* 36 (2006) 555–608.
- [28] D. Teschner, J. Borsodi, A. Wootsch, Z. Revay, M. Havecker, A. Knop-Gericke, S.D. Jackson, R. Schlögl, *Science* 320 (2008) 86–89.
- [29] A. Borodzinski, G.C. Bond, *Catal. Rev. Sci. Eng.* 48 (2006) 91–144.
- [30] M.P. Jigato, B. Coussens, D.A. King, *J. Chem. Phys.* 118 (2003) 5623–5634.
- [31] D.W. O'Sullivan, M.Y. Lee, B.C. Noone, B.G. Heikes, *J. Phys. Chem.* 100 (1996) 3241–3247.
- [32] M.J. Janik, C.D. Taylor, M. Neurock, *Top. Catal.* 46 (2007) 306–319.